INJURY BIOMECHANICS RESEARCH
Proceedings of the Forty First International Workshop

PMHS Thorax Response in Low- and High-Speed Oblique and Lateral Ram Impacts

Heather Rhule
National Highway Traffic Safety Administration

Brian Suntay, Rodney Herriott, and Jim Stricklin
Transportation Research Center Inc.

Yun-Seok Kang and John H. Bolte IV
The Ohio State University

This paper has not been screened for accuracy nor refereed by any body of scientific peers and should not be referenced in the open literature.

ABSTRACT

In 2011 Rhule et al. presented results from twelve PMHS impacted once each to the left side of the thorax at either 4.5 or 5.5 m/s in a pure lateral or 30° anterior oblique direction with a 23 kg pneumatic ram with a rectangular impact face at the level of the xyphoid process. Normalized responses at 4.5 m/s demonstrated similar characteristics for both lateral and oblique impacts, indicating that it may be reasonable to combine lateral and oblique responses together at this speed to define characteristic PMHS thoracic response as was done previously (ISO, 1999). However, the similarity in lateral and oblique thorax responses at injurious speed (4.5 m/s) differs from that found by Shaw et al. (2006) at sub-injurious speed (2.5 m/s). Shaw et al. conducted paired lateral and 30° anterior oblique thoracic impacts on opposite sides of seven PMHS at the level of the fourth intercostal space with a 23 kg pneumatic ram with a circular impact face. The data showed that oblique impacts resulted in more deflection and less force, whereas lateral impacts resulted in less deflection and more force. The current study presents results of 24 paired lateral and 30° anterior oblique thoracic impacts to five PMHS with a 23 kg pneumatic ram. The test matrix includes variations in vertical impact location (xyphoid vs. 4th intercostal space), impact speed (2.5 vs. 4.5 m/s), as well as impact face shape (rectangle vs. circle). Vertical impact location and impact speed did not appear to affect the lateral vs. oblique response trend; however, impact face shape did appear to affect the trend. All tests with the circular impact face resulted in stiffer lateral responses compared to oblique responses for a given subject, similar to the findings of Shaw et al. Most tests with the rectangular impact face resulted in similar

peak forces among paired lateral and oblique impacts for a given subject, similar to the findings of Rhule et al.

INTRODUCTION

In 2006 Shaw et al. presented results of PMHS tested at a sub-injurious speed of 2.5 m/s in lateral and 30° anterior to lateral pneumatic ram impacts to the thorax. Each PMHS was impacted twice: once laterally and once obliquely on opposite sides of the thorax to examine the difference in response between lateral and oblique impacts for each subject and among subjects. The mass of the ram was 23.86 kg and the aluminum impact face was a 152.4 mm (6 inch) diameter circle with a depth of 50.8 mm (2 inch) and an edge radius of 12.7 mm (0.5 inch). For each impact, the center of the ram was located at the vertical level of the fourth intercostal space with slight downward adjustments when necessary to ensure no arm interaction occurred with the ram. Shaw et al. found that at 2.5 m/s, the mean normalized lateral thoracic impact demonstrated a significantly stiffer response than the mean normalized 30° oblique thoracic impact.

In 2011 Rhule et al. presented results of PMHS tested at a potentially injurious speed of 4.5 m/s in pure lateral and 30° anterior to lateral (oblique) pneumatic ram impacts to the thorax. Each PMHS was impacted once on the left side, either in the lateral or oblique direction. The mass of the ram was 22.99 kg and the impact face was a rigid aluminum 152.4 mm vertical x 304.8 mm horizontal x 12.7 mm thick (6 x 12 x 0.5 inch) rectangular plate with a 3.175 mm (0.125 inch) edge radius. For each impact, the ram was centered vertically at the level of the xyphoid. No significant difference was found between the mean normalized response curves of lateral and oblique impact directions at 4.5 m/s. Figure 1 shows the mean normalized response curves with +/- 1 standard deviation biofidelity targets for the 2.5 m/s and 4.5 m/s lateral and oblique thoracic impacts presented by Rhule et al. (2011) with consistent deflection measurement, normalization and biofidelity response target generation methods.

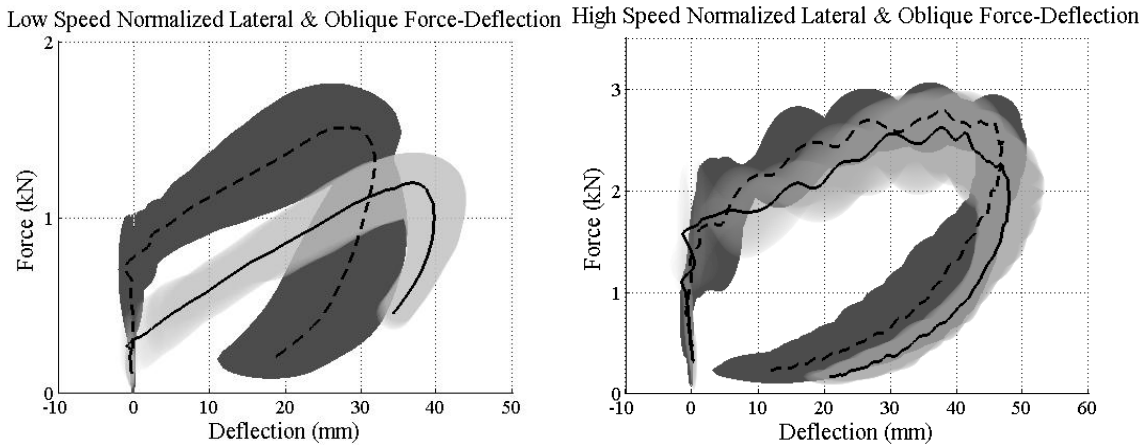

Figure 1. Mean normalized force-deflection response curves with +/- 1 standard deviation biofidelity targets for re-processed 2.5 m/s thoracic impact data of Shaw et al. (2006) (left) and 4.5 m/s thoracic impact data of Rhule et al. (2011) (right); lateral response targets shown in dark gray and oblique response targets shown in light gray.

Because the observed lateral vs. oblique response trends of the low-speed circular impactor tests of Shaw et al. and the high-speed rectangular impactor tests of Rhule et al. were different, further testing was warranted in order to examine why the response trends might be different. Objectives of the current study included the following:

- Conduct paired lateral and oblique thoracic impacts on five PMHS
- Examine effects of various test parameters such as
  - impact direction (lateral vs. oblique)
  - impact speed (2.5 vs. 4.5 m/s)
  - vertical impact location (fourth intercostal space vs. xyphoid) and

- impact face shape (152.4 mm dia. circle vs. 152.4 mm x 304.8 mm rectangle)
- Determine why previous lateral vs. oblique response trends in 2.5 and 4.5 m/s test conditions are different

METHODS

Test Matrix

In order to address the objectives, individual subjects were impacted in lateral and oblique directions multiple times with different test conditions, so that the effect of the various conditions on response from the same subject could be compared. Pneumatic ram impacts were conducted on the thorax of five PMHS at either 2.5 or 4.5 m/s. The ram was centered vertically at one of two locations, either at the xyphoid process or at the fourth intercostal space. The ram face was either a 152.4 x 304.8 x 12.7 mm (6 x 12 x 0.5 inch) rectangle with an edge radius of 3.175 mm (0.125 inch) and an impactor mass of 23.135 kg or a 152.4 mm (6 inch) diameter circle with a depth of 50.8 mm (2 inches), an edge radius of 12.7 mm (0.5 inch) and an impactor mass of 23.994 kg. For each impact speed, location and face shape combination, one lateral impact and one 30° anterior to lateral (oblique) impact were conducted per subject. The impact speed, vertical impact location and impact face were varied to examine the effects of the test parameters on the lateral vs. oblique impact response relationship of the PMHS. Table 1 shows the impact speed, location and face shape combinations and the subjects tested in each combination, with the test sequence, orientation and impact side denoted.

Table 1. Test Matrix

		Low-speed (2.5 m/s)						High-speed (4.5 m/s)					
		Impact Location						Impact Location					
		Xiphoid			4th			Xiphoid			4th		
		Subject	Impact Sequence/ Orientation	Impact Side	Subject	Impact Sequence/ Orientation	Impact Side	Subject	Impact Sequence/ Orientation	Impact Side	Subject	Impact Sequence/ Orientation	Impact Side
Impactor Shape	Rectangle	1101	1/Oblique	Left				1101	3/Oblique	Right			
			2/Lateral	Right					4/Lateral	Left			
		1201	1/Oblique	Right				1201	3/Oblique	Left			
			2/Lateral	Left					4/Lateral	Right			
		1203	1/Lateral	Right									
			4/Oblique	Left									
		1204	1/Oblique	Left									
			2/Lateral	Right									
	Circle	1202	2/Lateral	Right	1202	1/Lateral	Right				1202	5/Oblique	Left
			3/Oblique	Left		4/Oblique	Left					6/Lateral	Right
		1204	3/Lateral	Right	1203	2/Lateral	Right						
			4/Oblique	Left		3/Oblique	Left						

Subject Selection

PMHS were selected from the Anatomy Body Donation Program[1] at The Ohio State University based on the following guidelines:

[1] Research was reviewed and approved by the NHTSA and The Ohio State University Institutional Review Board (IRB) and was conducted in accordance with the practice of the IRB.

- No invasive surgery or other events that may have compromised the structural integrity of the thorax
- Not osteoporotic; Young adult T-score of -2.5 or above
- Body Mass Index between 18.5-29.9 (normal-overweight)
- Body mass of 95.3 kg or less (for ease of moving subject)

Unlike the 2011 study only male subjects were accepted for testing in order to reduce the variation in height and mass of subjects as well as to avoid the issue of interference of breast tissue.

Subject Preparation

Five fresh, unembalmed cadavers were prepared prior to testing. The subject's body was washed with antiseptic soap and a 10% bleach solution. Anthropometric measurements were taken while the subject was in a supine position and the subject was visually inspected for any scars or evidence that the structural integrity of the thorax was compromised. After passing the visual inspection, a bone mineral density (BMD) scan was performed on the subject using a DEXA scan machine. The Young Adult T-score was reported from the L2-L4 region of the spine because it is closest to the region of impact and is an accepted location to clinically define BMD. If the Young Adult T-Score was found to be acceptable, the subject underwent pre-test Computed Tomography (CT) scans to identify any pre-existing structural damage and as a baseline for post-test comparisons. Subjects were kept in a 4.4 °C (40°F) cooler for preservation overnight after instrumentation was installed prior to testing the following day.

Instrumentation

Two strain gages (Model # CEA-06-062UW-350 w/Option P2, Vishay Micro Measurements Group, Raleigh, NC) were installed on each rib in the region of impact for ribs 3-10 on the left and right sides of the rib cage to determine in which tests rib fractures occurred. Each rib was exposed with a three-inch long incision along the length of the rib and scraped clean of any soft tissue. Ether was applied in order to clean and dry the surface of each rib prior to gluing the strain gages. A 40-gage chest band was positioned on the subject at the level of impact (either the xyphoid or fourth intercostal space). Aluminum blocks instrumented with three linear uniaxial accelerometers and three angular rate sensors (3aω blocks) were installed on mounts at T4 on the spine and at the mid-sternum location to measure kinematic motion of the subject in the x, y, and z directions.

The pneumatic ram was instrumented with a linear accelerometer on the rear side of the impact face. Velocity of the ram was determined by integrating the ram acceleration and verified using a light trap. Initial three-dimensional positions of the locations of pertinent anatomical structures and instrumentation, the ram face center and the table on which the subject was seated were recorded with a FARO arm (FARO Technologies, Inc., Lake Mary, FL).

Test Performance

The subject was positioned at a distance from the pneumatic ram face such that impact with the subject would occur upon the ram reaching constant velocity. The subject was seated on a hydraulic lift table such that the impactor was centered vertically at either the level of the xyphoid or the fourth intercostal space and horizontally through the approximate center of gravity of the subject so as not to induce rotation of the thorax. For oblique impacts, the subject was rotated such that the impact occurred 30° anterior to lateral. The arms were positioned at approximately 90 degrees relative to the body and parallel to the floor, with the forearms crossed and supported by a strut. The head was fitted with a harness, which was hooked to a magnetic release suspended from a moveable track. The track was able to move in the anterior-posterior and in the medial-lateral directions so that proper alignment of the subject could be achieved.

A foam-padded structure was positioned behind and around the non-impact side of the subject in order to prevent the subject from falling over after the impact, but while allowing the subject to fully interact with the ram without being restricted by the foam-padded structure. The lungs were pressurized with approximately 45-60 cc of air through a vent tube in the trachea prior to impact. No pressurization of the

thoracic vasculature was performed. Figure 2 shows an oblique impact setup and a lateral impact setup with the rectangular impactor face centered at the level of the xyphoid prior to impact. Figure 3 shows a lateral impact setup with the circular impactor face centered at the level of the fourth intercostal space.

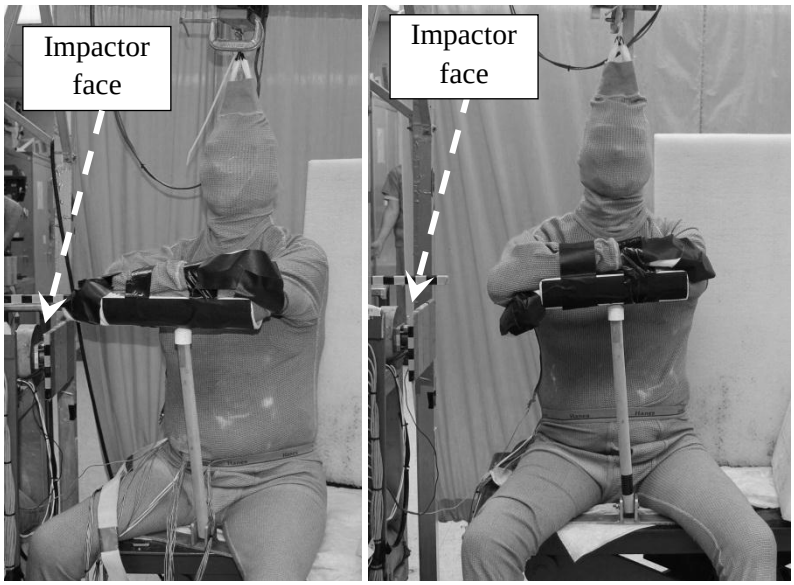

Figure 2. Pre-test photograph showing 30° oblique (left) and 0° lateral (right) setup with rectangular impactor face centered at the xyphoid

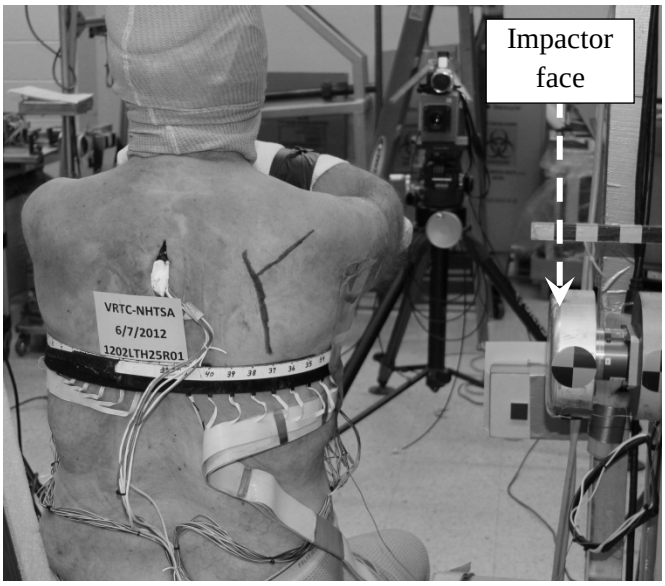

Figure 3. Pre-test photograph showing 0° lateral setup with circular impactor face centered at the fourth intercostal space

Tests performed with the ram face centered at the vertical location of the fourth intercostal space were conducted without long underwear on the subject's upper body so that potential interaction between the scapula and the ram face could be documented with high-speed video. Impact tests were conducted at the Injury Biomechanics Research Laboratory at The Ohio State University. High-speed digital video cameras recorded the event at 1000 frames/sec. Data was recorded on a 96-channel Yokogawa Electric Corporation WE7000 data acquisition system, with a sampling rate of 20,000 Hz.

Since multiple tests would be performed with each subject, the strain gages installed on the ribs were used to monitor the occurrence of rib fractures during each test. After each test was performed, the strain gage data was reviewed for a distinct drop in strain, which has been associated with rib fracture (Kemper, 2011). For tests where a subsequent test was to be performed on the same side of the rib cage, if the strain gage data showed more than two ribs fractured, then the subsequent test was not performed. For tests where a subsequent test was to be performed on the opposite side of the rib cage, and the data showed more than three ribs fractured, then the subsequent test was not performed.

Post-Test Imaging and Autopsy

A post-test CT scan was performed after the last test on each subject, followed by a detailed necropsy to identify injuries caused by the impacts. The necropsy included a complete anatomical dissection moving from superficial to deep for both the thoracic and abdominal cavities. The skin and subcutaneous tissue were removed and all muscles were dissected and any abnormalities were documented. Following the reflection of the muscles the skeleton was examined, which included cleaning all twelve sets of ribs, sternum, clavicles, and scapulae. The cavities were then opened and all internal organs in both the thoracic and abdominal cavities were checked for injury. Both sides of the subject were examined along with the intercostal spaces. The clavicles and scapulae were also examined for any damage. The AAAM Abbreviated Injury Scale 2005, Update 2008 (AAAM, 2008) was used to assign injury descriptive values (AIS scores).

Data Processing

Data of the current study was processed as in the Rhule 2011 study. Data processing included filtering impactor acceleration with a Channel Filter Class (CFC) 180 and calculating applied force by multiplying the measured ram linear acceleration by its mass. Chest band data was processed using CrashStar version 2.5 (NHTSA, 2010) to produce contours of the chest band shape at each point in time. Chest deflection was determined using the forced angle method. In the forced angle method, the distance is calculated between each gage on the chest band and a point along the spine-sternum line. The point, referred to as the origin, is located at half the initial chest depth (determined from the chest band gages) from the spine, along the spine-sternum line. Each gage-to-origin distance measurement is determined at each point in time and subtracted from the corresponding gage-to-origin distance established prior to the impact event. The gage on the contour which achieves the largest change in magnitude from its initial gage-to-origin distance determines the maximum deflection. The angle from the spine-sternum line to the line connecting each gage-to-origin is also measured at each point in time for each gage and the angle at which maximum deflection occurs is determined. Time zero was defined using the deflection vs. time curve from the chest band gage that measured maximum chest deflection. Time zero is defined as the last time at which deflection equals zero prior to reaching maximum deflection. For the purposes of this paper, the data was not normalized. The effective stiffness was calculated for each impact over the interval of zero deflection to maximum deflection as shown in Equation 1.

$$\int F dx = \frac{1}{2} k_{eff} \; x_{\max}^2 \Rightarrow k_{eff} = \frac{2\int F dx}{x_{\max}^2} \qquad [1]$$

where:

x = thoracic displacement from chest band and k_{eff} = effective stiffness of thorax.

RESULTS

Subject Characteristics

Table 2 lists the characteristics of the subjects tested in the current study. All subjects were male, between the ages of 21 and 76 years old, with a height between 172 and 183.5 cm and a body mass between 67.5 and 97.5 kg. Although one subject's body mass was outside the subject selection guidelines, all other subject characteristics were within the guidelines. Chest breadth and chest depth ranged from 269.5 to 351 mm and 165.5 to 255 mm, respectively.

Table 2. Subject characteristic data

Subject	Gender	Age	Height (cm)	Body Mass (kg)	Body Mass Index (kg/m^2)	Young-Adult T-Score	Chest Breadth (mm)*	Chest Depth (mm)
1101	Male	21	173.0	67.5	22.6	-1.6	269.5	165.5
1201	Male	56	176.0	88.0	28.4	1.6	332.0	234.0
1202	Male	76	183.5	97.5	29.0	1.4	342.5	241.5
1203	Male	71	172.0	75.8	25.6	3.0	315.0	225.0
1204	Male	75	183.0	92.1	27.5	-0.1	351.0	255.0
	Min	21.0	172.0	67.5	22.6	-1.6	269.5	165.5
	Max	76.0	183.5	97.5	29.0	3.0	351.0	255.0
	Avg	59.8	177.5	84.2	26.6	0.9	322.0	224.2
	Std Dev	20.7	4.9	11.0	2.3	1.6	28.9	31.0

*average of measurements at axilla and xyphoid while subject in supine position without chest band installed

Injuries

Table 3 shows the injuries sustained in each impact for each subject. As shown in Table 3, the majority of injuries sustained during testing included transverse, non-displaced rib fractures at the anterior location of the rib. Only one subject (1101) did not sustain any injuries. Subject 1201 sustained one left rib fracture during the third impact (first high speed test on left side), followed by three right ribs fractured during the fourth impact (first high speed test on right side). Subject 1202 sustained fractures to left ribs 6-10, but it is not known whether these occurred during the third, fourth, and/or fifth impact. Since fractures to left ribs 3-5 occurred during the fifth impact (first high-speed impact to left side), it is suspected that fractures to left ribs 6-10 also occurred during this test. However, due to issues with the strain gages on left ribs 6-10, there is no data to show when these fractures occurred. In addition, subject 1202 sustained three right rib fractures during the sixth impact (first high speed test on right side). Subject 1203 sustained one left rib fracture during the third test and a fracture to an additional left rib during the fourth test. Subject 1204 sustained a fracture to one left rib during the first test and fractures to two additional left ribs during the fourth test. The fractures sustained by subjects 1203 and 1204 occurred during low speed tests.

Table 3. Injury results

Subject #	Impact Speed (m/s)	Impact Location	Impact Face	Impact Side	Orientation	Test Sequence	Fx'd Ribs	Fractured Rib Locations and Type of Fracture		AIS Score (AAAM 2005, '08 update)	AIS description (AAAM 2005, '08 update)
								Anterior	Posterior		
1101	2.5	X	R	L	O	1				n/a	n/a
	2.5	X	R	R	L	2				n/a	n/a
	4.5	X	R	R	O	3				n/a	n/a
	4.5	X	R	L	L	4				n/a	n/a
1201	2.5	X	R	R	O	1					
	2.5	X	R	L	L	2					
	4.5	X	R	L	O	3	L5	trans., NDS		450201.1	Fractures without flail, 1 rib
	4.5	X	R	R	L	4	R5	trans., NDS		450203.3	Fractures without flail, ≥3 ribs
							R6	trans., H-shaped, NDS			
							R7	trans., NDS			
1202	2.5	4	C	R	L	1				n/a	n/a
	2.5	X	C	R	L	2				n/a	n/a
	2.5	X	C	L	O	3	**	**	**	**	**
	2.5	4	C	L	O	4	**	**	**	**	**
	4.5	4	C	L	O	5	**	**	**	**	**
							L3	trans., NDS		450203.3	Fractures without flail, ≥3 ribs
							L4	trans., DS	trans., NDS		
							L5	trans., DS	trans., DS		
	4.5	4	C	R	L	6	R8	trans., NDS		450203.3	Fractures without flail, ≥3 ribs
							R9	trans., DS			
							R10	trans., NDS			
1203	2.5	X	R	R	L	1				n/a	n/a
	2.5	4	C	R	L	2				n/a	n/a
	2.5	4	C	L	O	3	L4	trans., NDS		450201.1	Fractures without flail, 1 rib
	2.5	X	R	L	O	4	L5	trans., DS		450201.1	Fractures without flail, 1 rib
1204	2.5	X	R	L	O	1	L6	trans., NDS		450201.1	Fractures without flail, 1 rib
	2.5	X	R	R	L	2					
	2.5	X	C	R	L	3					
	2.5	X	C	L	O	4	L4	trans., NDS		450202.2	Fractures without flail, 2 ribs
							L5	trans., NDS			

Orientation: O – 30° oblique; L – lateral		NDS: nondisplaced	
Impact side: L – left; R – right		DS: displaced	gray shade: oblique test
Impact location: X – xyphoid; 4 – 4th intercostal space		H-shaped: 2 parallel hairline fractures in communication	
Impact face:geometry: R – rectangle ; C – circle		trans.: transverse - across the long axis	

**Could not determine which test or tests these fx occurred in due to strain gage issues (L6, L8, L9, L10 trans., NDS; L7 trans., DS)

Lateral Vs. Oblique Response Comparisons

Five combinations of impact speed, impact location and impact face were tested. Table 4 shows the peak non-normalized force and deflection and effective stiffness values for each test. For tests with the rectangular impact face (white cells in Table 4), peak forces were similar in paired oblique and lateral impacts for four out of six cases: 1101, 1201, 1204 xyphoid, low speed and 1101xyphoid, high speed. For two subjects tested with the rectangular face, peak forces were less in oblique impacts compared to lateral impacts for a given subject (see **bold** in Table 4; 1203 xyphoid, low speed and 1201 xyphoid, high speed). For all but one test with the rectangular face, the deflection in the oblique impact was greater than that in the lateral impact for a given subject, although the difference in deflection between oblique and lateral tests per subject only ranged from 2.8 to 8.5 mm. For all tests with the circular impact face (gray cells in Table 4), peak forces were less (17- 32%) and peak deflections were greater (18-95%) per subject in oblique compared to lateral impacts.

Table 4. Lateral vs. oblique peak force, deflection and effective stiffness values

Test Parameters for Comparison	Subject	Impact Side	Orientation	Test Sequence	# Ribs Fx'd	# Ribs Fx'd on same side before this test?	Peak Non-normalized Force (N)	Peak Non-normalized Deflection (mm)	Effective Stiffness (N/mm)
Rectangle, Xyphoid, Low speed	1101	L	O	1			1225.2	19.3	106.3
		R	L	2			1207.1	10.8	196.9
	1201	R	O	1			1685.8	**22.6**	117.2
		L	L	2			1603.1	**26.4**	89.0
	1203	L	O	4	1	1	**1200.2**	30.1	67.8
		R	L	1			**1461.3**	27.3	89.2
	1204	L	O	1	1		1229.1	30.4	66.9
		R	L	2			1319.5	24.3	87.1
Rectangle, Xyphoid, High speed	1101	R	O	3			2597.3	37.2	118.5
		L	L	4			2686.8	28.7	163.9
	1201	L	O	3	1		**2631.7**	44.3	107.7
		R	L	4	3		**3580.5**	39.5	132.9
Circle, Xyphoid, Low speed	1202	L	O	3	**		1170.6	63.3	25.3
		R	L	2			1555.4	33.9	57.0
	1204	L	O	4	2	1	1019.8	27.6	60.1
		R	L	3			1229.8	22.9	86.2
Circle, 4th intercostal, Low speed	1202	L	O	4	**	**	962.2	46.6	29.5
		R	L	1			1420.1	30.5	76.9
	1203	L	O	3	1		1045.0	60.6	27.0
		R	L	2			1472.9	31.1	66.3
Circle, 4th intercostal, High speed	1202	L	O	5	3**	**	2342.4	63.1	39.9
		R	L	6	3		3304.6	53.3	97.7

Impact side: L – left; R – right

Orientation: O – 30° oblique; L – lateral

** 5 ribs fractured on subject 1202; not known in which test(s) they occurred (#3, 4, and/or 5)

Tests with circular impact face

Figures 4a-4f show lateral and oblique force-deflection responses for the various combinations of test parameters. Subjects are distinguished by line color. Impact orientation is distinguished by line thickness (thick = oblique impacts; thin = lateral impacts). Impacts with the circular impactor face are shown in the left column and impacts with the rectangular impactor face are shown in the right column. Figures 4a-4c show that, for each subject, the lateral response is stiffer than the oblique response when the circular impact face is used. Figures 4d-4f do not show a clear lateral vs. oblique response trend for the subjects impacted with the rectangular impact face, although most tests demonstrated similar peak forces for paired lateral and oblique impacts per subject.

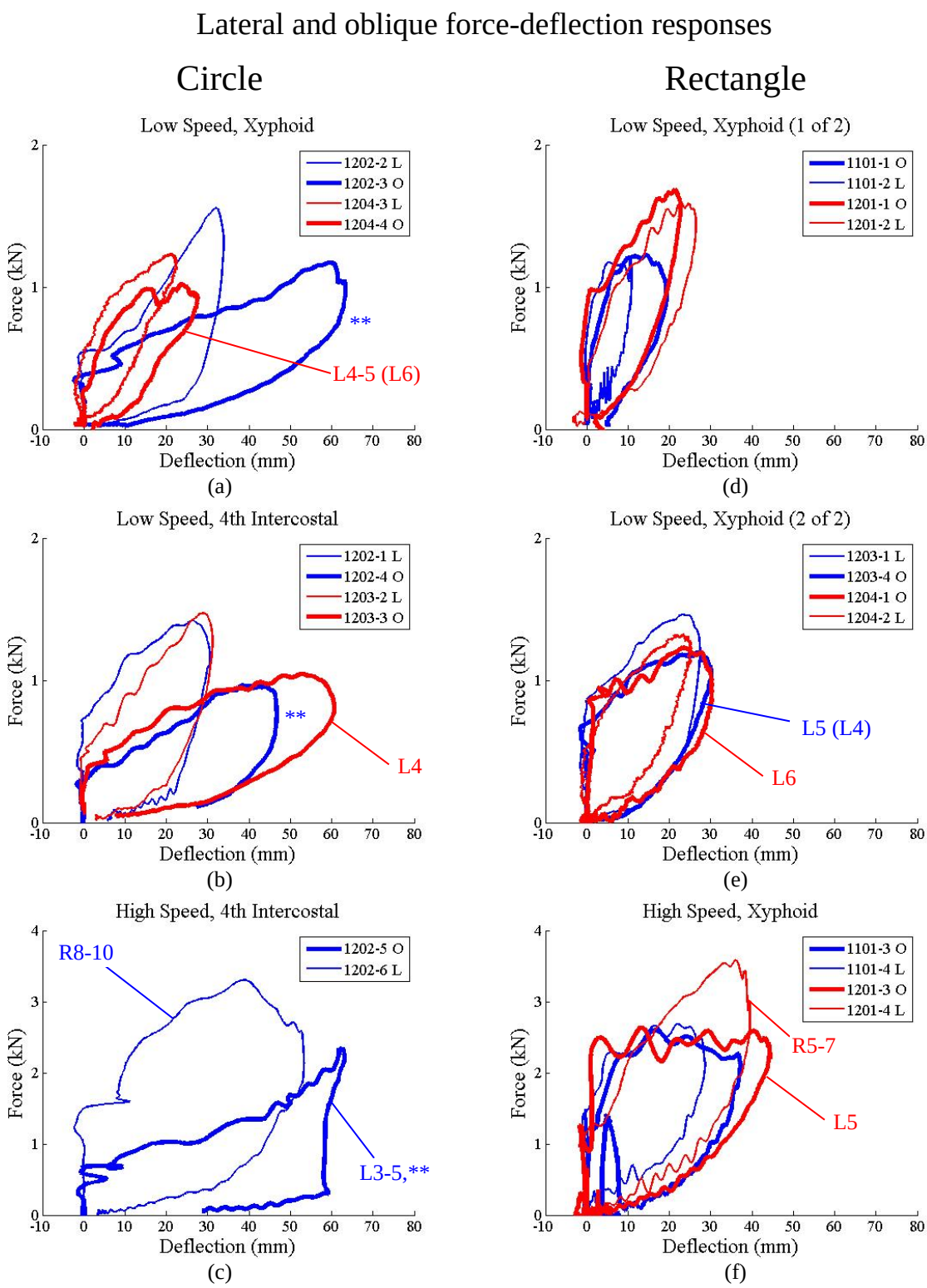

Figure 4. Lateral and oblique force-deflection responses for each combination of impact speed, location, and face shape. Impacts with circle are shown in left column and impacts with rectangle are shown in right column. Ribs fractured are shown for tests in which fractures occurred, but not necessarily at the deflection at which they occurred, with fractures in parenthesis indicating ribs previously fractured. **indicates left ribs 6-10 fractured in test 1202-3, 1202-4, and/or 1202-5.

DISCUSSION

This study investigates why the lateral vs. oblique mean normalized force-deflection response curves with +/- 1 standard deviation biofidelity targets are different between the low-speed tests conducted by Shaw et al. at the fourth intercostal space with a circular impact face and high-speed tests conducted by Rhule et al. at the xyphoid with a rectangular impact face. Test parameters including vertical impact location, impact speed, and impact face shape were varied for multiple paired lateral and oblique tests to try to ascertain why the lateral vs. oblique response trends in the previously mentioned conditions are different.

Injuries

Because individual subjects were used as a control to remove the variation due to human subject variability and to be able to directly compare lateral vs. oblique responses in various conditions, the occurrence of injuries should be considered with respect to the objective. For the purposes of this paper, it was assumed that one or two rib fractures would not affect the force-deflection response enough to change the lateral vs. oblique response trend. Subject 1202 had questionable injury results due to problems with the strain gages in tests 3, 4, and 5. However, Figures 4a and 4b show that the other subjects that were tested in the same configurations as subject 1202 at low speed demonstrated similar lateral vs. oblique response relationships, indicating that either the rib fractures did not occur in tests 3 and 4, or that the fractures did not affect the lateral vs. oblique response relationship. At high speed, no other subjects were tested in the same configuration as subject 1202, so there is no other data to know if the lateral vs. oblique response relationship was driven by the rib fractures or by the test condition. Thus, these rib fractures only limit the conclusions made regarding subject 1202 at high speed. Although subject 1201 sustained three rib fractures during its fourth test – high-speed lateral with the rectangle at the xyphoid - the peak force from this test was 950 N higher than in the paired oblique test (test 3). If the rib fractures had not occurred in test 4, the peak force would still have been higher than that of the oblique test 3, which would have given the same lateral vs. oblique response relationship seen in Figure 4f.

Vertical Impact Location

Rhule et al. (2011) speculated that the superior vertical impact location of the fourth intercostal space in the Shaw et al. (2006) tests might have had an effect on the lateral response being stiffer due to the scapula and musculature that exists higher on the thorax and that would interact with the impactor in lateral impacts, but not oblique impacts. The effect of the vertical impact location on the lateral vs. oblique response trend is illustrated in Figures 4a and 4b where subjects were impacted with the circular impact face at low speed and only the vertical impact location was varied. (Note that subject 1202 was impacted at both vertical locations.) As the lateral response is stiffer than the oblique response per subject, whether impacted at the fourth intercostal space or the xyphoid, it appears that the vertical impact location does not affect the lateral vs. oblique response trend at low speed, even though videos from tests with the impact location at the fourth intercostal space did show scapular involvement.

Impact Speed

The effect of impact speed on the lateral vs. oblique response trend is illustrated in Figures 4b and 4c where subjects were impacted with the circular impact face at the fourth intercostal space and only the impact speed was varied, and in Figures 4d, 4e and 4f where subjects were impacted with the rectangular impact face at the xyphoid and only the impact speed was varied. Figures 4b and 4c show each subject demonstrating stiffer lateral responses vs. oblique responses, and Figures 4d, 4e and 4f show there is no clear lateral vs. oblique response trend at low- or high-speed. These results suggest that the impact speed does not appear to affect the lateral vs. oblique response trend. However, it should be noted that the responses of subject 1202 (Figure 4c) and subject 1201 (Figure 4f) could have been affected by the multiple rib fractures sustained in the high speed tests. As these impacts were conducted at high speed, it will be difficult to ascertain the answer to the question regarding the effect of impact speed on the lateral vs. oblique response relationship since it is likely that rib fractures will occur at this speed. From these results, it is suggested, but not clearly proven, that impact speed does not appear to affect the lateral vs. oblique response trend.

Impact Face Shape

The effect of impact face shape on the lateral vs. oblique response trend is illustrated in Figures 4a, 4d, and 4e, where subjects were impacted at the xyphoid at low speed and only the impact face shape was varied. Figure 4a shows each subject demonstrating stiffer lateral responses vs. oblique responses with the circular impact face, whereas Figures 4d and 4e show no clear lateral vs. oblique response trend with the rectangular impact face. It should be noted that the impacts with the rectangular face were only conducted at the xyphoid and that subject 1204 was impacted with both impact face shapes (Figures 4a and 4e). However, given the results of the effect of vertical location on the lateral vs. oblique response trend, limiting the comparison to xyphoid impacts should not matter.

Figures 4a and 4e show responses for subject 1204, which was impacted with the circular and rectangular impact faces at low speed at the xyphoid. The impacts with the circular face show a stiffer lateral response as compared to the oblique response. The impacts with the rectangular face show similar peak forces but more deflection in the oblique impact. In all impacts with the circular impact face (Figures 4a-4c), lateral responses are consistently stiffer than oblique responses per subject. In most impacts with the rectangular impact face (Figures 4d-4f), peak forces in paired lateral and oblique impacts are similar, but peak deflections vary. These results indicate that the impact face shape affects the lateral vs. oblique response trend, where the circular shape results in a stiffer lateral response and the rectangular shape results in similar peak forces with varying amounts of deflection.

In order to determine if the mean effective stiffness values were statistically different between paired lateral and oblique impacts with the circle at low speed, a paired t-test was performed. The null hypothesis was chosen so that the mean difference in effective stiffness values for lateral and oblique impacts was zero. The level of significance was set at $\alpha = 0.05$. Table 5 shows the t, t_{crit} and p values and the result of the t-tests. The results in Table 5 show that the t value (7.8) was more than the critical t value (3.2), and the p value (.004) was less than 0.05, indicating that the null hypothesis should be rejected and that there is a significant difference between the mean lateral and oblique effective stiffness values for subjects impacted with the circle at low speed. A second paired t-test was performed for lateral and oblique impacts with the rectangle at low speed to determine if the mean effective stiffness values were statistically different. Again, the null hypothesis was chosen so that the mean difference in effective stiffness values for lateral and oblique impacts was zero and the level of significance was set at $\alpha = 0.05$. Table 5 shows that the null hypothesis should be accepted and that there is no significant difference between the mean lateral and oblique effective stiffness values for subjects impacted with the rectangle at low speed. Thus, it appears that the impact face shape <u>does</u> affect the lateral vs. oblique response trend at low speed. Rhule et al. (2011) found that a significant difference exists between the mean lateral and oblique effective stiffness values for subjects impacted with the circle at the fourth intercostal space at 2.5 m/s, and a significant difference does not exist between the mean lateral and oblique effective stiffness values for subjects impacted with the rectangle at the xyphoid at 4.5 m/s. The results shown in Table 5 reiterate the findings of Rhule et al. as well as identify the apparent cause for the difference in lateral vs. oblique response trends – impactor face shape.

Table 5. T-test results

Test Condition	Comparison	t	t_{crit}	p	null hypothesis	Result
CIRCLE - Low speed (2.5 m/s)	lateral vs. oblique effective stiffness	7.8112	3.1824	0.0044	mean difference = 0	Reject null hypothesis
RECTANGLE - Low speed (2.5 m/s)	lateral vs. oblique effective stiffness	1.0645	3.1824	0.3652	mean difference = 0	Accept null hypothesis

Due to the larger area of the rectangular face, it is suspected that its <u>full</u> area might not engage the subject in both lateral and oblique impacts, whereas with the smaller circular face, its full area most likely does engage the subject in both lateral and oblique impacts (Figure 5). Tests with the smaller (circular) face would have a consistent load distribution for both lateral and oblique impacts, but tests with the larger (rectangular) face might not. For example, because the rectangular face is wider than the subject, when the impactor engages the subject, a varying amount of the impact face will interact with the subject in each direction, depending on the size, shape, contour, stiffness, etc., of the subject. Because the area of the larger

(rectangular) impactor which engages the subject may not be consistent between lateral and oblique impacts of a given subject, resulting in variation in load distribution between the two impact directions, this impact face may not be ideal for examining the difference in response between lateral and oblique impacts Perhaps, in addition to the fact that the area of the larger (rectangular) impactor which engages the subject may not be consistent between lateral and oblique impacts of the same subject, affecting the direct comparison of lateral to oblique responses, a larger impact area (compared to the 150 mm diameter circle) may elicit a more similar response in lateral vs. oblique impacts, due to the more distributed load. A small impact face size relative to the size of the thoracic area to be impacted produces significantly different lateral vs. oblique responses, which may be due to the difference in curvature of the ribs in the lateral and oblique impact locations.

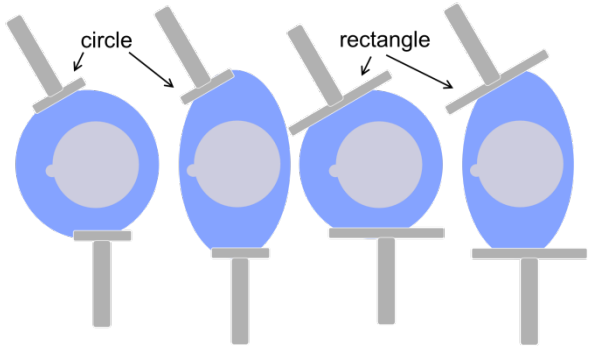

Figure 4. Schematic illustrating possible impactor face engagement with subject, where oblique impacts are shown at the top of the figure and lateral impacts are shown at the bottom, for two different subjects, each with a circular and rectangular impact face

Although the sample sizes were small, multiple impacts were conducted on individual subjects, and strain gage failures prevented determination of when some rib fractures occurred, the implications of this study are that the vertical impact location of xyphoid vs. fourth intercostal space and possibly the impact speed of 2.5 vs. 4.5 m/s do not greatly affect the lateral vs. oblique force-deflection response relationship. However, the relative size of the impact face does affect the lateral vs. oblique force-deflection response trend in low- and high-speed impacts. Finally, the mean lateral and oblique responses and +/- 1 standard deviation biofidelity targets presented by Shaw et al. and Rhule et al. are valid for the test conditions employed. Because there is not a significant difference between the mean effective stiffness values in lateral vs. oblique impacts with the rectangle at low- or high-speed, lateral and oblique responses could be grouped together to form one biofidelity response target for each speed. Although ISO grouped normalized lateral and oblique responses together to form a force-time biofidelity response corridor because the peak forces were similar, the impactor used was a 150 mm diameter circle, as used here and by Shaw et al. It is not known why the lateral and oblique normalized peak force responses used by ISO would have been similar, which is not consistent with the findings here.

CONCLUSIONS

The following bullets summarize the conclusions of this study.

- Based on tests where only vertical impact location was varied, it appears that the vertical impact location does not affect the lateral vs. oblique response trend.
- Based on tests where only impact speed was varied, it appears that the impact speed does not affect the lateral vs. oblique response trend.
- Impact face size affects the lateral vs. oblique response trend, where the smaller impactor (circle) results in a stiffer lateral response and the larger impactor (rectangle) results in similar peak forces with varying amounts of deflection.
- Because there is not a significant difference between the mean effective stiffness values in lateral vs. oblique impacts with the rectangle at low- or high-speed, lateral and oblique responses could be grouped together to form one biofidelity response target for each speed

REFERENCES

ASSOCIATION FOR THE ADVANCEMENT OF AUTOMOTIVE MEDICINE. (2008) Abbreviated Injury Scale © 2005, Update 2008. Association for the Advancement of Automotive Medicine, Barrington, IL.

EPPINGER, R.H., MARCUS, J.H., MORGAN, R.M. (1984) Development of Dummy and Injury Index for NHTSA's Thoracic Side Impact Protection Research Program. SAE paper number 840885. Proc. SAE Government/Industry Meeting and Exposition, Pp 983-1011. Society of Automotive Engineers, Warrendale, PA.

INTERNATIONAL STANDARDS ORGANIZATION (ISO) (1999) Road vehicles – Anthropomorphic Side Impact Dummy – Lateral Impact Response Requirements to Assess the Biofidelity of the Dummy. ISO/TR 9790:1999(E).

KEMPER, A.R., KENNEDY, E.A., MCNALLY, C., MANOOGIAN, S.J., STITZEL, J.D., DUMA, S.M. (2011) Reducing Chest Injuries in Automobile Collisions: Rib Fracture Timing and Implications for Thoracic Injury Criteria. *Annals of Biomedical Engineering*, Vol. 39, No. 8

NATIONAL HIGHWAY TRAFFIC SAFETY ADMINISTRATION. (2010) CrashStar – A Post-processing Program For Chestband Data Analysis – Draft User's Manual. Available upon request from heather.rhule@dot.gov.

PINTAR, F., HUMM, J., YOGANANDAN, N., MARTIN, P. (2009) Test Program To Define Oblique Chest Loading In Side Impact. The 21st International Technical Conference on the Enhanced Safety of Vehicles, Washington D.C.

RHULE, H., SUNTAY, B., HERRIOTT, R., AMENSON, T., STRICKLIN, J., BOLTE, J. (2011) Response of PMHS to High- and Low-Speed Oblique and Lateral Pneumatic Ram Impacts. *Stapp Car Crash Journal* Vol. 55.

SHAW, J., HERRIOTT, R., MCFADDEN, J., DONNELLY, B., BOLTE, J. (2006) Oblique and Lateral Impact Response of the PMHS Thorax. *Stapp Car Crash Journal* Vol. 50.

VIANO, D. (1989) Biomechanical Response and Injuries in Blunt Lateral Impact. SAE paper number 892432. Proc. 33rd Stapp Car Crash Conference, Society of Automotive Engineers, Warrendale, PA.

YOGANANDAN, N., HUMM, J., PINTAR, F., BRASEL, K., RUDD, R., RIDELLA, S. (2012) Thoraco-abdominal Deflection Responses of Post Mortem Human Surrogates in Side Impacts. *Stapp Car Crash Journal* Vol. 56.

Appendix

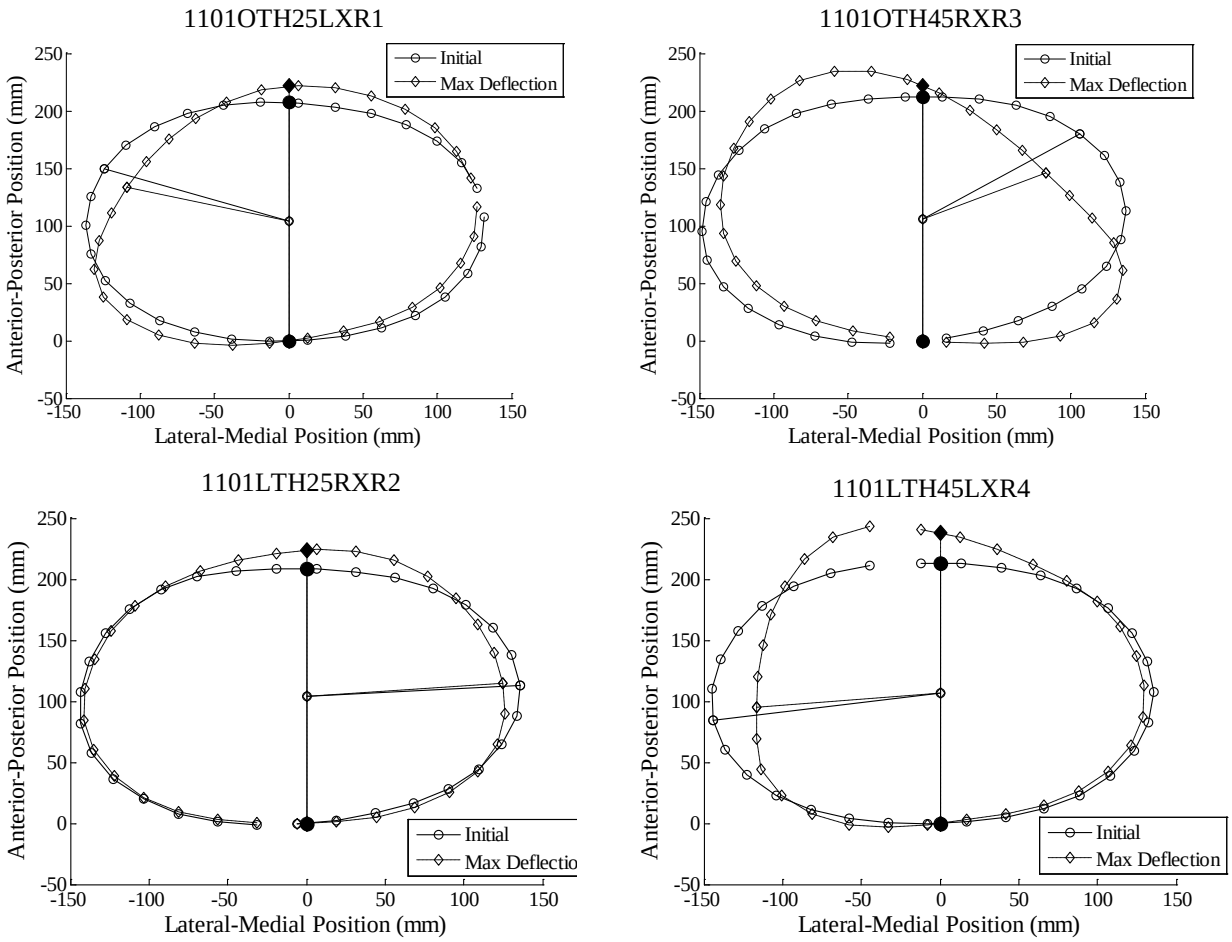

Figure A1. Chest band contours for subject 1101.

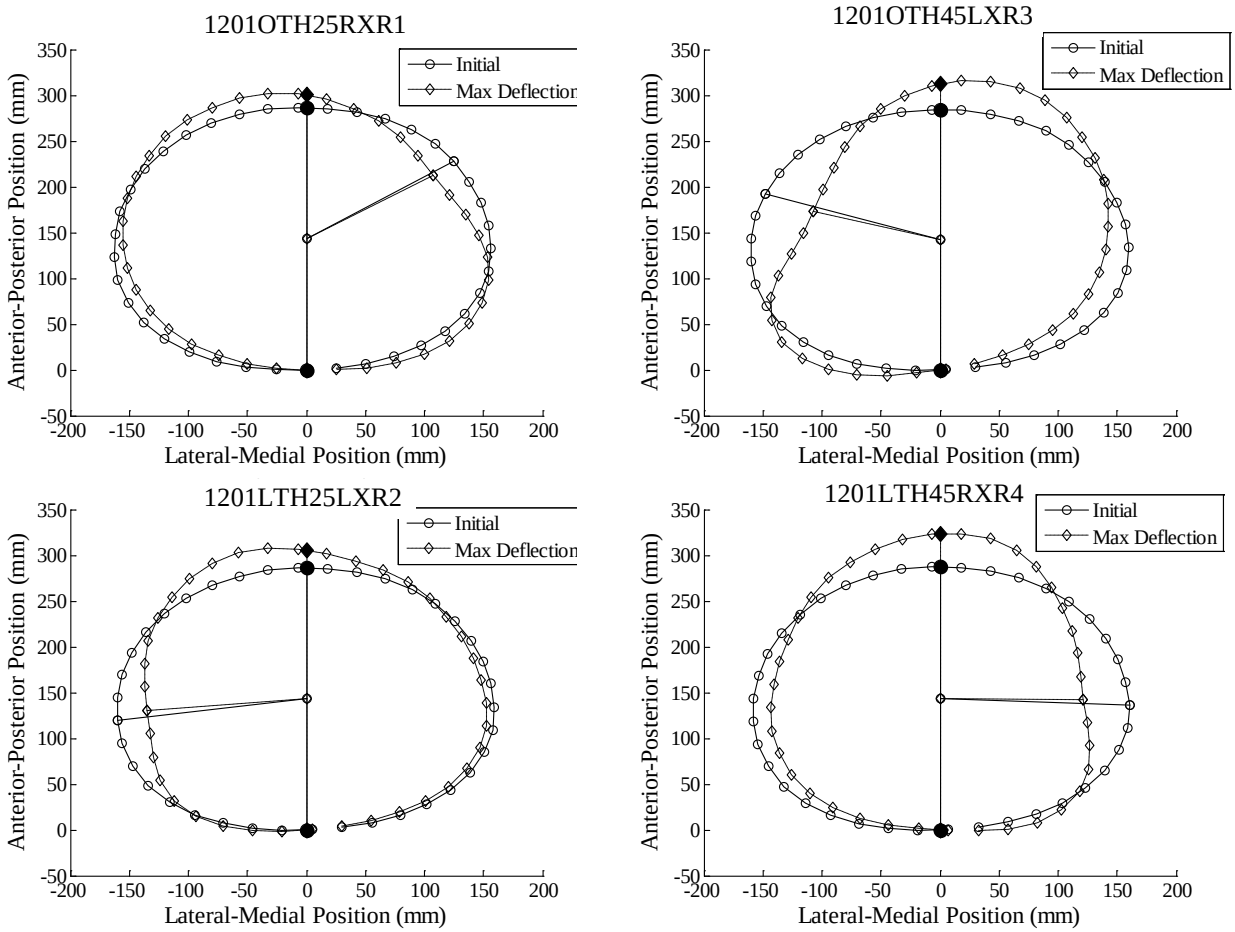

Figure A2. Chest band contours for subject 1201

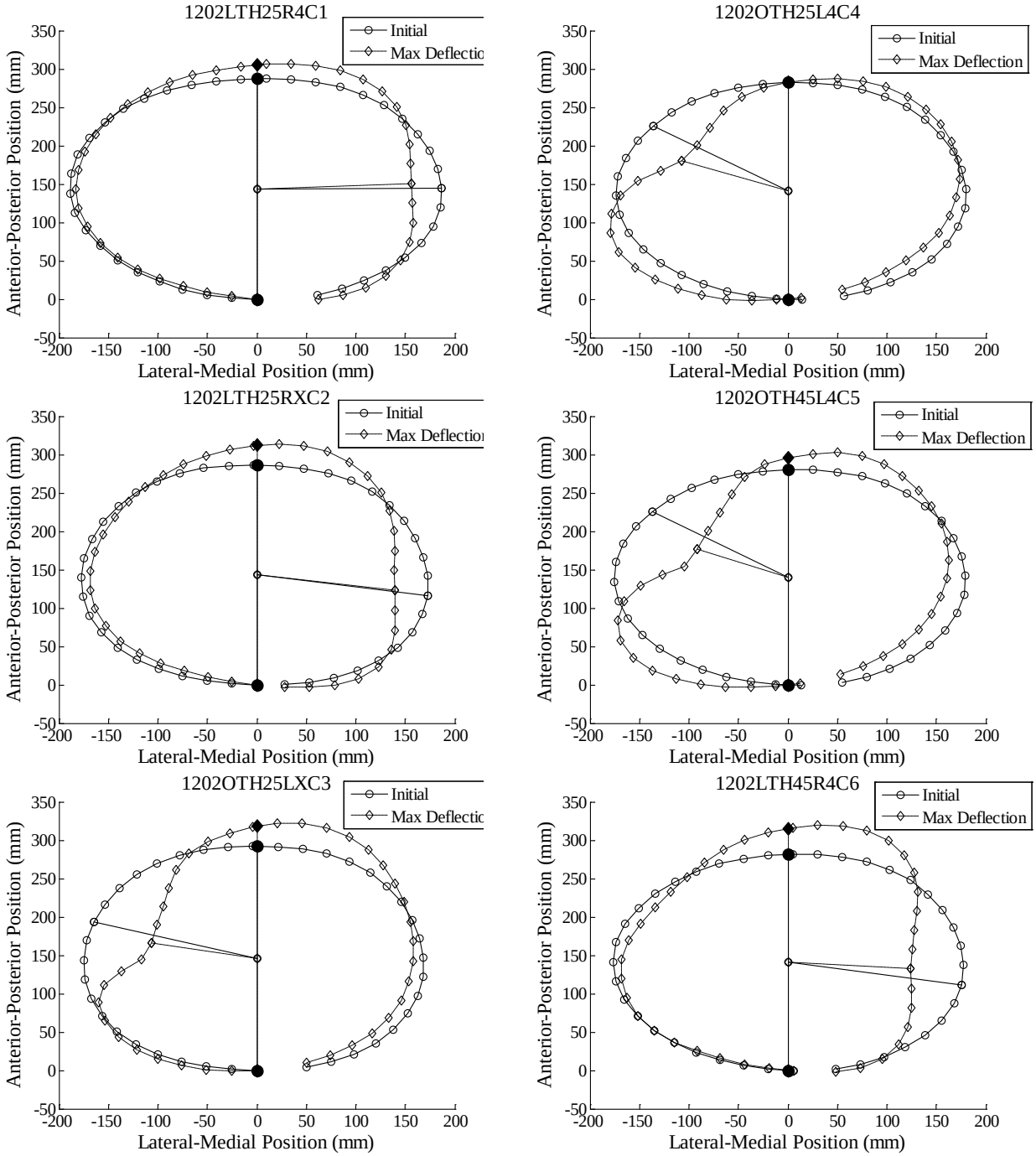

Figure A3. Chest band contours for subject 1202

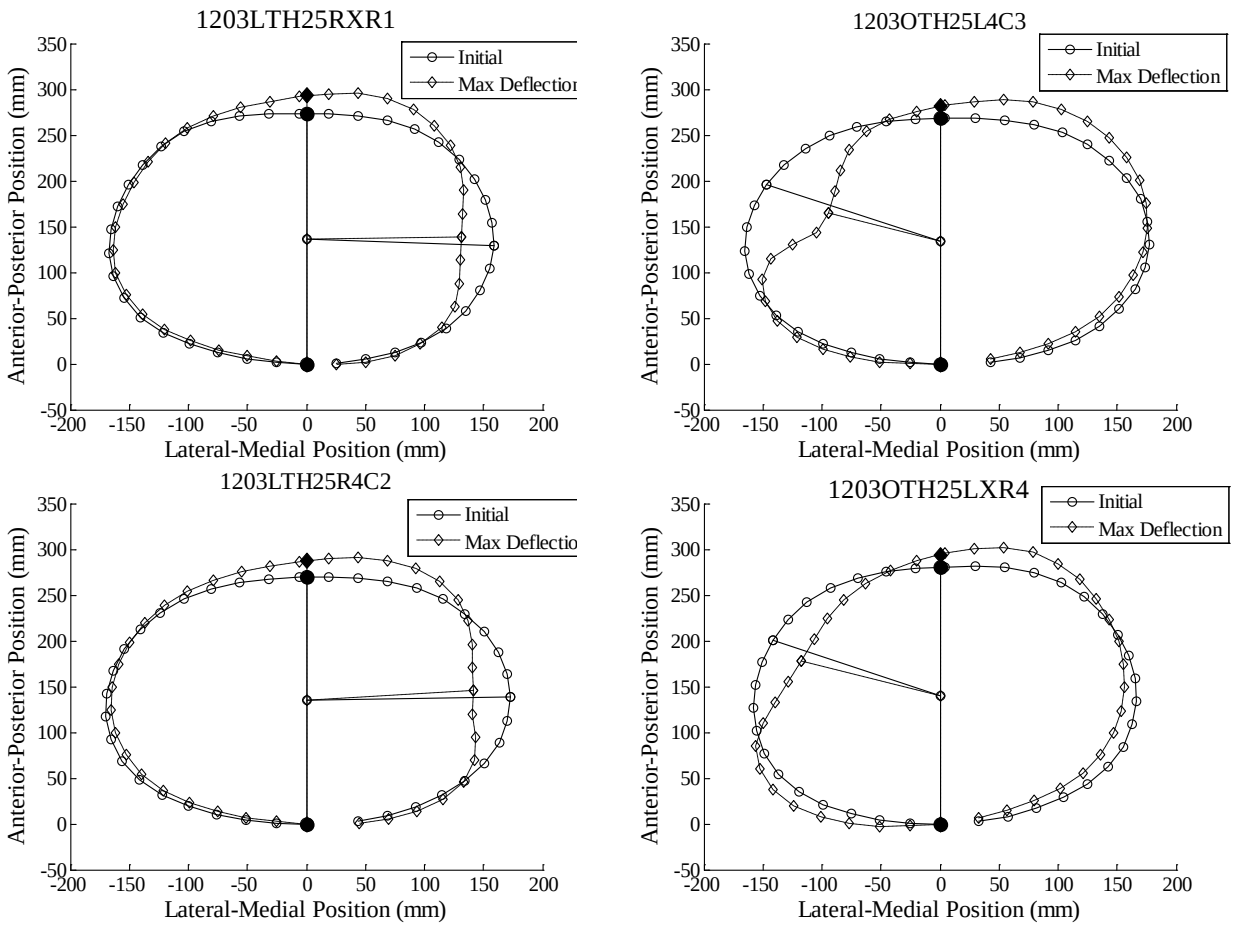

Figure A4. Chest band contours for subject 1203

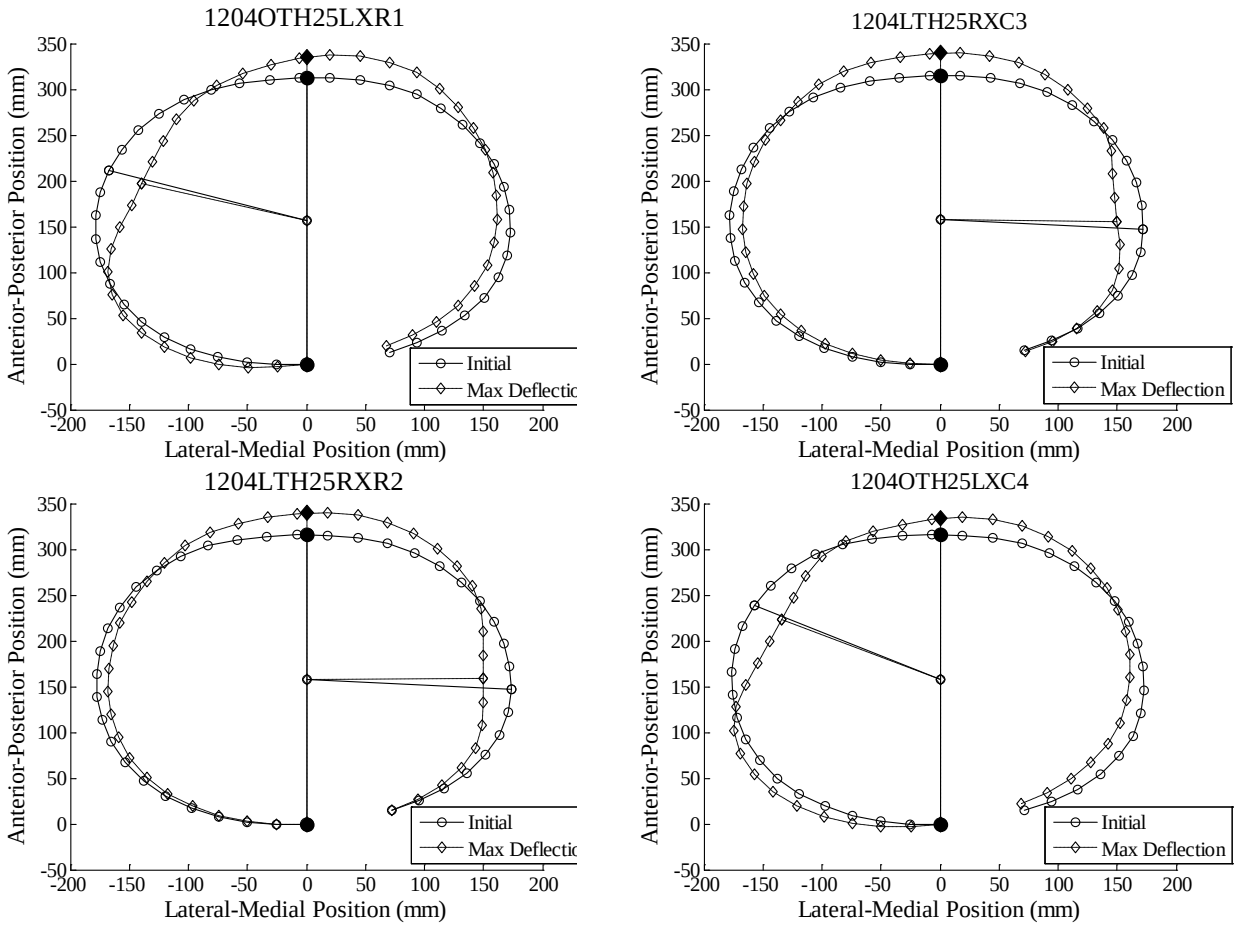

Figure A5. Chest band contours for subject 1204

Table A1 lists the non-normalized maximum half chest deflection and angle of maximum chest deflection from the spine-sternum line for each impact.

Table A1. Non-normalized maximum half chest deflection and angle of maximum chest deflection

Subject	Test #	Non-normalized Max Half-Chest Deflection (mm)	Angle of Max Deflection from Spine-Sternum Line (deg)
1101	1101OTH25LXP1	19.3	74.5
	1101LTH25RXP2	10.8	85.1
	1101OTH45RXP3	37.2	64.6
	1101LTH45LXP4	28.7	95.7
1201	1201OTH25RXP1	22.7	57.3
	1201LTH25LXP2	26.4	95.3
	1201OTH45LXP3	44.3	73.9
	1201LTH45RXP4	39.5	90.7
1202	1202LTH25R4C1	30.5	87.4
	1202LTH25RXC2	33.9	98.2
	1202OTH25LXC3	63.3	79.3
	1202OTH25L4C4	46.6	70
	1202OTH45L4C5	63.1	68
	1202LTH45R4C6	53.3	94
1203	1203LTH25RXP1	27.3	89.1
	1203LTH25R4C2	31.1	85.6
	1203OTH25L4C3	60.3	72
	1203OTH25LXP4	30.1	71.9
1204	1204OTH25LXP1	30.4	73.8
	1204LTH25RXP2	24.3	89.7
	1204LTH25RXC3	22.9	90.6
	1204OTH25LXC4	27.3	64.1